No significant variations were observed in the three check reflections during data collection. A numerical absorption correction was applied to the data on the crystal faces (010, 0$\bar{1}$0), (110, $\bar{1}$10), (1$\bar{1}$0, $\bar{1}$10), (10$\bar{1}$, $\bar{1}$01), and (001, 00$\bar{1}$) (transmission factors 0.886 (max) and 0.734 (min)). The intensity data were converted to F_o after correction for Lorentz and polarization effects.

Structure Solution and Refinement. The systematic absences uniquely define the space group as $P2_1/n$. The positions of the Co atoms were determined by centrosymmetric direct methods (EEES: SHELX 76).[31] The remaining non-hydrogen atoms were located from subsequent electron density difference syntheses. The structure was refined by blocked full-matrix least squares with Co, P, O, and acetylenic and carbonyl C atoms anisotropic. The phenyl rings were treated as rigid groups (d(C–C) = 1.395 Å; ∠(C–C–C) = 120°), and the phenyl H atoms were placed in idealized positions (d(C–H) = 1.08 Å) and allowed to ride on the relevant carbons; the H atoms were assigned a common isotropic temperature factor. The weighting scheme (Table III) was introduced and gave reasonable agreement analyses. The maximum shift/error in the final cycle of refinement was 0.02, and a difference electron density synthesis showed features only in the range +0.93 to −0.58 Å^{-3}. The final R value is 0.061 for 3827 observed data ($F_o > 5\sigma(F_o)$) for 291 parameters. Atomic scattering factors for neutral atoms and anomalous dispersion corrections were taken from ref 32 and SHELX 76[31] (P, O, C, H). All calculations were performed with use of programs in ref 31. Final atomic coordinates and equivalent isotropic displacement parameters are listed in Table IV.

Theoretical Calculations. Fenske–Hall molecular orbital calculations[33] were carried out on $Co_4(CO)_{10}(HC_2H)$ (1) with use of crystallographically determined coordinates.[5b] The calculations employed a single-ζ Slater function for the 1s and 2s functions of C and O. The exponents were obtained by curve fitting the double-ζ function of Clementi;[34] double-ζ functions for the 2p orbitals were used directly. An exponent of 1.16 was used for H. The Co 1s and 3d functions[35] were chosen for the 1+ oxidation state and were assigned by 4s and 4p functions with exponents of 2.00.

Acknowledgment. We thank the Council of National Research (CNR, Rome) and the MURST (Rome) for financial support. C.N. thanks the European Economic Community (EEC) for a studentship grant within the ERASMUS scheme.

Supplementary Material Available: Anisotropic displacement parameters (Table S1), hydrogen atom coordinates and isotropic displacement parameters (Table S2), and tables of bond distances and angles for 4 (4 pages); a table of observed and calculated structure factors for 4 (22 pages). Ordering information is given on any current masthead page.

(31) Sheldrix, G. M. *SHELX 76, Program for Crystal Structure Determination*; University of Cambridge: Cambridge, 1976.
(32) *International Tables for X-ray Crystallography*; Kynoch Press: Birmingham, England, 1974; Vol. 4, pp 91–161, 149–150.
(33) Fenske, R. F.; Hall, M. B. *Inorg. Chem.* **1972**, *11*, 768.
(34) Clementi, E. *J. Chem. Phys.* **1964**, *40*, 1944.
(35) Richardson, J. W.; Nieuwpoort, W. C.; Powell, R. R.; Edgell, W. F. *J. Chem. Phys.* **1962**, *36*, 1057.

Thermodynamic and Kinetic Stability of Bis(η^3-allyl)bis(μ_2-η^3-allyl)- and Bis(η^3-methallyl)bis(μ_2-η^3-methallyl)dimolybdenum(II) Isomers and Evidence for Their Lewis Base Catalyzed Isomerization

Reed J. Blau,* Mary S. Goetz, Ronda R. Howe, Cheri J. Smith, and Rong-Jer Tsay

Department of Chemistry, University of Texas at Arlington, Arlington, Texas 76019

Upali Siriwardane

Department of Chemistry, Southern Methodist University, Dallas, Texas 75275

Received December 3, 1990

The reactivity of $Mo_2(\mu_2\text{-}\eta^3\text{-allyl})_2(\eta^3\text{-allyl})_2$ (1) is dependent on the conformation of the bridging allyls. The green Mo_2(*endo*-μ_2-η^3-allyl)(*exo*-μ_2-η^3-allyl)(*endo*-η^3-allyl)$_2$ (1(b=en,ex)(t=en$_2$)) reacts much more rapidly than the violet Mo_2(*endo*-μ_2-η^3-allyl)$_2$(endo-η^3-allyl)$_2$ (1(b=en$_2$)(t=en$_2$)) with a variety of reagents including methanol, acetylacetone, and carbon monoxide. In fact, the violet isomer can be isolated from an isomeric mixture of $Mo_2(\mu_2\text{-}\eta^3\text{-allyl})_2(\eta^3\text{-allyl})_2$ via titration with methanol. 1(b=en$_2$)(t=en$_2$) crystallizes in the orthorhombic space group *Pbcn* with cell constants a = 8.275 (11) Å, b = 11.832 (7) Å, c = 12.862 (9) Å, V = 1259 (2) Å^3, Z = 8, and $R(F)$ = 3.01%. A comparison of crystal structures for 1(b=en,ex)(t=en$_2$) and 1(b=en$_2$)(t=en$_2$) shows significantly shorter Mo–C bonds involving the terminal allyls of the latter isomer. 1(b=en$_2$)(t=en$_2$) is isomerized to an equilibrated mixture of isomers upon the addition of a Lewis base catalyst. A comparison of COSY data for various isomers of 1 and $Mo_2(\mu_2\text{-}\eta^3\text{-methallyl})_2(\eta^3\text{-methallyl})_2$ (2) suggests that 2 exists primarily as the 2(b=en,ex)(t=en,ex) isomer (88%) with minor amounts of 1(b=en,ex)(t=ex$_2$) also present (12%).

Since the report of its discovery in 1966,[1] tetraallyldimolybdenum, $Mo_2(\mu_2\text{-}\eta^3\text{-allyl})_2(\eta^3\text{-allyl})_2$ (1), has been utilized as a precursor in the formation of catalysts for olefin[2] and alkyne metathesis,[3] propene and ethanol oxidation,[4] and the polymerization of a variety of olefins including butadiene[5] and methyl methacrylate.[6] Most recently, catalysts have been prepared by the chemisorption

(1) Wilke, G.; Bogdanović, B.; Hardt, P.; Heimbach, P.; Keim, W.; Kröner, M.; Oberkirch, W.; Tanaka, K.; Steinrücke, E.; Walter, W.; Zimmerman, H. *Angew. Chem., Int. Ed. Engl.* **1966**, *5*, 151.
(2) Ermakov, Y. I.; Kuznetzov, B. N.; Grabovskii, Y. P.; Startzev, A. N.; Lazutkin, A. M.; Zakharov, V. A.; Lazutkina, A. I. *J. Mol. Catal.* **1976**, *1*, 93.
(3) Mortreux, A.; Petit, F.; Blanchard, M. *J. Mol. Catal.* **1980**, *8*, 97.
(4) Iwasawa, Y. In *Tailored Metal Catalysts*; Iwasawa, Y., Ed.; Reidel Publishing Co., Member Kluwer Academic Publishers Group: Boston, MA, 1986; Chapter 1.
(5) Skoblikova, V. I.; Passova, S. S.; Babitskii, B. D.; Kormer, V. A. *Vysokomol. Soedin., Ser. B* **1968**, *10*, 590.
(6) Ballard, D. G. H.; Janes, W. H.; Medinger, T. *J. Chem. Soc. B* **1968**, 1168.

0276-7333/91/2310-3259$02.50/0

of 1 on inorganic oxide support surfaces. Many of these latter catalysts have been characterized stoichiometrically and spectroscopically, and much is known about the structure and function of their active sites.[4,7]

Research devoted to elucidating the structural complexities of 1 and its reactivity in the homogeneous phase[8,9] have progressed much more slowly. The crystal structure of an important isomeric form was reported by Cotton et al. 1971.[10] This very reactive Mo(II) dimer is unique in that its four allylic ligands are coordinated through two different bonding modes: two π-allyls are bridging the Mo–Mo quadruple bond with each π-allyl in the remaining pair binding to a single molybdenum atom. Both of the terminal allyls are coordinated in an endo conformation with respect to each other and the Mo–Mo quadruple bond. The bridging allyls are coordinated in a cis fashion about the Mo–Mo bond axis with one found in an exo and the other in an endo configuration. Thus, this isomer can be named more specifically $Mo_2(\mu_2\text{-}\eta^3\text{-}endo\text{-allyl})(\mu_2\text{-}\eta^3\text{-}exo\text{-allyl})(\eta^3\text{-}endo\text{-allyl})_2$ (1(b=en,ex)(t=en$_2$)).

Considering all possible combinations of terminal allyl conformations and bridging allyl configurations, nine isomers of 1 are possible. In 1981, the characterization of 1 in benzene-d_6 via ^{1}H NMR spectroscopy was reported by Benn et al.[11] The above-mentioned isomer, 1(b=en,ex)(t=en$_2$), was found to be equilibrated with an additional

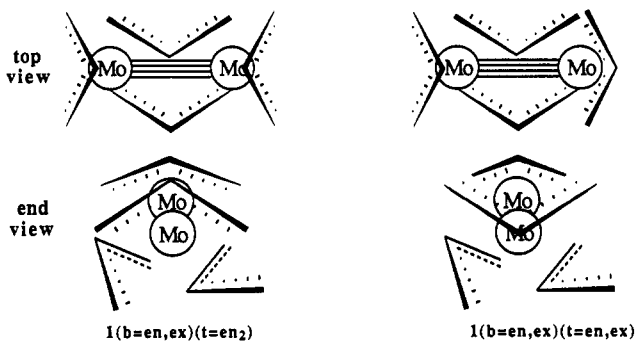

isomer, 1(b=en,ex)(t=en,ex), at a nine to one ratio. Interconversion of these two isomers was detected at 80 °C by way of ^{1}H NMR magnetization transfer. During our investigations into the reactivity of 1, we have discovered and characterized an additional isomer of 1, which differs markedly from the two previously known isomers in its reactivity with a variety of reagents. These results as well as the two-dimensional ^{1}H NMR characterization of $Mo_2(\mu_2\text{-}\eta^3\text{-methallyl})_2(\eta^3\text{-methallyl})_2$ (2) will be reported. Substitution of the allylic ligands by methallyls, $[CH_2CMeCH_2]^-$, causes a significant perturbation in the distribution of isomers found in solution.

Results and Discussion

Isolation and Characterization of 1(b=en$_2$)(t=en$_2$). Typically, known synthetic routes to 1 yield isomeric mixtures that are green to blue-green in color. Solutions in which 1 is reacting with one of a variety of reagents including alcohols, phenols, silanols, β-diketones, ketones, carbon monoxide, or water undergo ofttimes a color transition from green to violet before attaining the color of the final product(s). The violet species does not correspond to a metastable intermediate, since careful titration of 1 with less than stoichiometric amounts of the above reagents yields solutions in which the violet color is persistent. In fact, the violet species can be isolated in a pure form by using titrants such as methanol or salicyclic acid, which react preferentially with the green isomers of 1 forming products that are completely insoluble in hydrocarbon solvents.

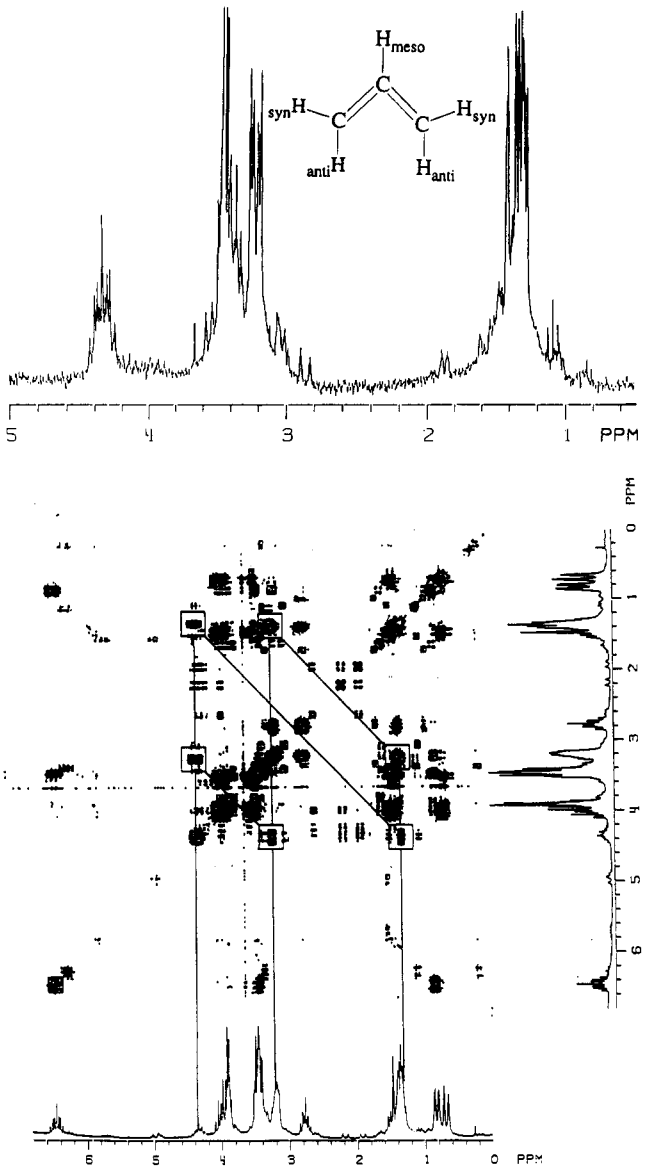

Figure 1. (a) Top: ^{1}H NMR spectrum of 1(b=en$_2$)(t=en$_2$) in benzene-d_6 at 200 MHz. The resonances corresponding to the meso, anti, and syn protons of the endo-bridging allyls are found at 4.37 (multiplet), 3.20 (doublet of doublets), and 1.34 ppm (doublet of doublets), respectively. The resonance at 1.42 ppm corresponding to the anti protons of the endo-terminal allyls appears as a simple doublet whereas the syn (3.46 ppm) and meso (3.38 ppm) resonances exhibit a more complex splitting pattern due to a second-order effects. (b) Bottom: ^{1}H–^{1}H COSY spectrum in benzene-d_6 at 200 MHz of an equilibrium mixture of 1 isomers with the crosspeak pattern attributable to the endo-bridging allyls of 1(b=en$_2$)(t=en$_2$) highlighted.

The ^{1}H NMR spectrum of this violet species is simpler than that of 1(b=en,ex)(t=en$_2$) or 1(b=en,ex)(t=en,ex) due to a higher degree of symmetry (see Figure 1a). Violet hexagonal platelets that were formed via selective crystallization from a reaction solution derived from the titration of 1 with carbon monoxide were utilized in obtaining a crystal structure of this species (see Figure 2). This violet-colored compound is actually a heretofore undetected isomer of 1, $Mo_2(\mu_2\text{-}\eta^3\text{-}endo\text{-allyl})_2(\eta^3\text{-}endo\text{-allyl})_2$

(7) Candlin, J. P.; Thomas, H. In *Homogeneous Catalysis-II*, Forster, D., Roth, J. F., Eds.; Advances in Chemistry Series 132; American Chemical Society: Washington, DC, 1974; Chapter 15.
(8) Blau, R. J.; Goetz, M. S.; Tsay, R.-J. *Polyhedron* **1991**, *10*, 605.
(9) Blau, R. J.; Siriwardane, U. *Organometallics* **1991**, *10*, 1627.
(10) Cotton, F. A.; Pipal, J. R. *J. Am. Chem. Soc.* **1971**, *93*, 5441.
(11) Benn, R.; Rufinska, A.; Schroth, G. *J. Organomet. Chem.* **1981**, *217*, 91.

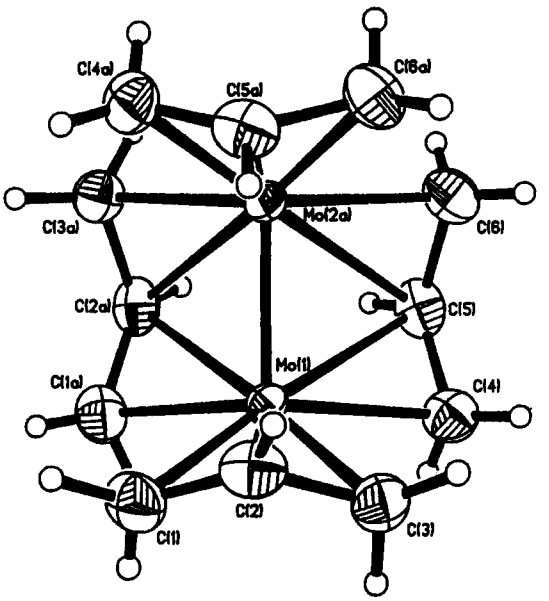

Figure 2. Crystal structure of 1(b=en_2)(t=en_2). Bond lengths and angles are summarized in Table I.

(1(b=en_2)(t=en_2)), belonging to the C_{2v} point group. Its bond distances and angles will be discussed later.

Lewis Base Catalyzed Isomerization of 1(b=en_2)(t=en_2). Since the presence of 1(b=en_2)(t=en_2) had not been reported previously, it was postulated initially that this violet isomer was formed solely via the Lewis base catalyzed isomerization in eq 1. More specifically, it was

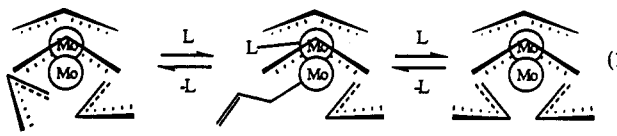

(1)

postulated that an external ligand induces a μ_2-η^3-*exo*-allyl to η^1-allyl transformation in 1(b=en,ex)(t=en_2). This is followed by rotation about the η^1-allyl Mo–C bond. Finally, a transformation of the η^1-allyl into the additional μ_2-η^3-*endo*-allyl that is prerequisite to the formation of 1(b=en_2)(t=en_2) occurs with the concomitant displacement of the catalytic Lewis base. Formation of violet 1(b=en_2)(t=en_2) exclusively via this catalytic route requires this isomer to be thermodynamically most stable.

A closer perusal of ^{1}H NMR spectra provides evidence for the presence of 1(b=en_2)(t=en_2) in the initial isomeric mixture of 1 before the addition of further reactants or potential isomerization catalysts. This violet isomer may not have been detected previously because all the multiplets corresponding to its ^{1}H NMR spectrum are intermingled with those of 1(b=en,ex)(t=en_2) and/or 1(b=en,ex)(t=en,ex). Thus, the presence of violet 1(b=en_2)(t=en_2) in the initial isomeric mixture of 1 is substantiated most convincingly through the ^{1}H–^{1}H COSY of this mixture (see Figure 1): intense cross peaks are observed at positions predicted by ^{1}H NMR homodecoupling experiments conducted on the isomerically pure violet 1(b=en)(t=en_2). In fact, various methods of integration suggest a 7:2:1 1(b=en,ex)(t=en_2):1(b=en_2)(t=en_2):1(b=en,ex)(t=en,ex) ratio of 1 isomers in samples that were synthesized from the reaction of Mo_2(acetate)$_4$ with allylMgCl.[7] However, these data do not ascertain whether additional violet isomer is produced during the reaction of 1 with potential isomerization catalysts.

The total insolubility of products formed from the reaction of methanol with 1 was exploited to determine if, parallel to this reaction, methanol catalyzes the formation of additional violet 1(b=en_2)(t=en_2) from the green isomers via eq 1. Isomer ratios of 1 were determined via ^{1}H NMR integration before and after the addition of 0.16 equiv of methanol. The percentage of violet isomer increased from 25% before to 31% of 1 that remained after the methanol was consumed. This is consistent with the selective reaction of 1 equiv of methanol with 1 equiv of the green isomers, 1(b=en,ex)(t=en_2) and 1(b=en,ex)(t=en,ex). The weight of insoluble product was also consistent with this stoichiometry. Thus, methanol reacts selectively with only the green isomers of 1 and does not catalyze the formation of additional violet isomer.

Similar conclusions can be reached by analysis of the reaction of carbon monoxide with 1, which occurs according to eq 2, forming light yellow to colorless products.[9] The

$$Mo_2(\mu_2\text{-}\eta^3\text{-}C_3H_5)_2(\eta^3\text{-}C_3H_5)_2 + 8CO \rightarrow 2Mo(CO)_4(\eta^4\text{-}1,5\text{-hexadiene}) \quad (2)$$

green to violet transition is observed in this reaction after the addition of 6 equiv of carbon monoxide. This observation is consistent with the 8:2 ratio of green to violet isomers found before reaction via integration of NMR resonances. The amount of violet isomer never exceeds that present at the beginning of the reaction.

The addition of pyridine or bis(diphenylphosphino)methane to an isomerically pure solution of violet 1(b=en_2)(t=en_2) at ambient temperature induces its isomerization to what is evidently the equilibrated ratio of isomers, 7:2:1 1(b=en,ex)(t=en_2):1(b=en_2)(t=en_2):1(b=en,ex)(t=en,ex) ratio, also observed in newly synthesized samples of 1. The half-life for the accompanying violet to green transition is approximately 30 min. In the absence of Lewis base, no evidence for the isomerization of the violet 1(b=en_2)(t=en_2) to green 1(b=en,ex)(t=en_2) is observed even over a period of days. Thus, external ligand-catalyzed isomerization does indeed occur as depicted in eq 1 with the equilibrium favoring the green 1(b=en,ex)(t=en_2) instead of the violet 1(b=en_2)(t=en_2). As opposed to carbon monoxide[9] and PMe_2Ph,[12] which react irreversibly with 1, the addition of pyridine or bis(diphenylphosphino)methane to 1 does not even cause a significant broadening of the reactant ^{1}H NMR resonances, signaling a very weak and reversible interaction. However, the reaction of isomerically pure violet 1(b=en_2)(t=en_2) with carbon monoxide proceeds directly to Mo(CO)$_4$(η^4-1,5-hexadiene) in eq 2 without being isomerized to 1(b=en,ex)(t=en_2). Thus, the rate of CO-catalyzed isomerization of 1(b=en_2)(t=en_2) to 1(b=en,ex)(t=en_2) is much slower than the rate of the reactions represented by eq 2.

Origin of the Kinetic Inertness of 1(b=en_2)(t=en_2) Relative to 1(b=en,ex)(t=en_2). The green to violet transition in the reactions of 1 with Brønsted–Lowry acids, carbonylated organics, or carbon monoxide cited above occurs because the violet 1(b=en_2)(t=en_2) is much less reactive kinetically than the major green isomer, 1(b=en,ex)(t=en_2), even though the latter is more stable thermodynamically. At least in the case of Brønsted–Lowry acids[8,13] and carbonylated organics,[14] the *terminal allyls* of 1 are attacked preferentially over their bridging counterparts. The most obvious difference between these two isomers is that the *bridging allyls* of 1(b=en_2)(t=en_2) are both in an endo configuration while those of 1(b=en,ex)(t=en_2) are endo and exo, respectively (see Figure 3).

(12) Blau, R. J. Unpublished results.
(13) Blau, R. J.; Hill, P. L.; Smith, C. J.; Tsay, R.-J.; Zhang, H. M. To be submitted for publication.
(14) Blau, R. J.; Howe, R. R.; Smith, C. J.; Ho, S.-I. Unpublished results.

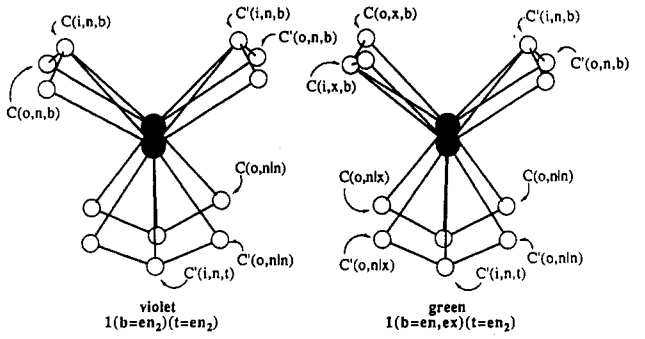

Figure 3. Ball and stick models of 1(b=en_2)(t=en_2) and 1(b=en,ex)(t=en_2) derived from crystallographic data including the positional parameters for 1(b=en,ex)(t=en_2) found in ref 10. See Table I for a comparison of bond lengths and angles. The abbreviations denote the following: i = inner or meso carbon; o = outer or methylenic carbon; n = part of an *endo*-allyl; x = part of an *exo*-allyl; b = part of a bridging allyl; t = part of a terminal allyl; |n = methylenic carbon of a terminal allyl closest to the endo-bridging allyl; |x = methylenic carbon of a terminal allyl closest to the exo-bridging allyl.

Table I. Structural Comparisons between 1(b=en_2)(t=en_2) and 1(b=en,ex)(t=en_2)

interatomic distance or angle[a]	violet 1(b=en_2)(t=en_2)[b]	green 1(b=en,ex)-(t=en_2)[b,c]
Mo–Mo, Å	2.162 (3)	2.183 (2)
bridging allyl		
Mo–C(o), Å	2.331 (2)	2.23 (2)
Mo–C(i), Å	2.614 (17)	2.51 (2)
C(o)–C(i), Å	1.383 (16)	1.37 (3)
terminal allyl		
Mo–C(o), Å	2.233 (7)	2.30 (3)
Mo–C(i), Å	2.226 (13)	2.33 (3)
C(o)–C(i), Å	1.383 (16)	1.37 (3)
Mo–Mo–C(i), deg	104.9 (0.9)	109 (1)
interbridging allyl		
C(i,n or x)–C'(i,n), Å	3.296 (9)	3.40 (3)
C(o,n or x)–C'(o,n), Å	3.998 (19)	3.46 (3)
av of two preceding values, Å	3.65	3.43 Å
C(i,n or x)–Mo–C'(i,n), deg	78.1 (0.1)	85 (1)
C(o,n or x)–Mo–C'(o,n), deg	118.1 (1.2)	102 (1)
av of two preceding values, deg	98.1	94
interterminal allyl		
C(i,n)–C'(i,n), Å	3.296 (9)	3.66 (3)
C(o,n|n)–C'(o,n|n), Å	3.998 (19)	4.52 (3)
C(o,n|x)–C'(o,n|x), Å	NA	4.26 (3)
weighted av of three previous values, Å	3.65	4.02 Å
other inter-allyl		
C(o,n|n)–C'(o,n,b), Å	3.02 (5)	3.09 (3)
C(o,n|x)–C(o,x,b), Å	NA	3.35 (3)

[a] See Figure 3 for an explanation of the abbreviations found in the parentheses. [b] Reported errors are the larger of either the average esd's accompanying each bond length/angle or the standard deviation of the bond lengths/angles from their average. [c] Data are derived from positional parameters found in ref 10.

We postulate that the kinetic inertness of 1(b=en_2)(t=en_2) can be explained by comparing interatomic distances and bond lengths and angles in the two structures: (1) The terminal allyls are bound more tightly to molybdenum in 1(b=en_2)(t=en_2); i.e., the terminal allyl Mo–C(o) and Mo–C(i) bond distances are significantly shorter for the violet 1(b=en_2)(t=en_2) than they are for green 1(b=en,ex)(t=en_2) (see Table I). (2) The terminal allyls in 1(b=en_2)(t=en_2) are more sterically shielded by its bridging allyls.

Steric shielding of the terminal allyls by their bridging counterparts is suggested by the significant steric compression of the terminal allyls toward each other in the violet 1(b=en_2)(t=en_2). For example, the inter-allyl distances between opposing carbons of the two terminal allyls

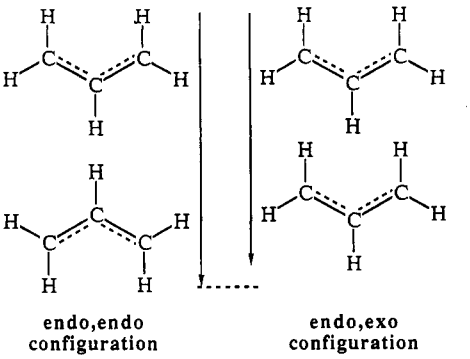

Figure 4. Comparison of the endo,endo and endo,exo configurations of the bridging allyls in 1(b=en_2)(t=en_2) and 1(b=en,ex)(t=en_2), respectively. All bond distances and the interatomic distances, C(i,n)–C'(i,n) and C(i,x)–C'(i,n), of 3.29 (2) and 3.40 (3) Å, respectively, are drawn to scale in order to illustrate the inefficiency of packing inherent in the endo,endo configuration of bridging allyls.

are, on the average, 0.37 Å shorter in the violet 1(b=en_2)(t=en_2) than in 1(b=en,ex)(t=en_2). The Mo–Mo–C(i,t) angles are also 4° smaller. This steric compression may be a result of two types of added interligand repulsions in the former: (a) inefficient packing of bridging allyls in the endo,endo configuration relative to those in the endo,exo configuration and (b) less efficient intermeshing of endo-*terminal* allyls with *endo*-bridging allyls than with their *exo*-bridging alternatives. Figure 4 illustrates the greater packing efficiency of the endo,exo configuration of the cis-oriented bridging allyls in green 1(b=en,ex)(t=en_2) described in (a): the V-shaped carbon skeletons of the allylic ligands intermesh. This is substantiated by the fact that the interatomic distances and angles between opposing carbon atoms of the two bridging allyls are, on the average, 0.22 Å shorter and 4° smaller, respectively, in the green isomer (see Table I). The packing inefficiency described in (b) is illustrated by the fact that the interatomic distances between the methylenic carbon atoms of *endo* bridging allyls and endo terminal allyls, C(o,n|n)–C'(o,n,b), are 0.3 Å shorter than the corresponding distances between methylenic carbons of *exo*-bridging allyls and endo terminal allyls, C(o,n|x)–C'(o,x,b) (compare Table I). Thus, inefficiencies in packing of the endo,endo configuration of bridging allyls in 1(b=en_2)(t=en_2) may cause a shielding of its terminal allyls from reagent attack increasing its kinetic stability relative to 1(b=en,ex)(t=en_2).

Origin of the Thermodynamic Stability of 1(b=en,ex)(t=en_2) Relative to 1(b=en_2)(t=en_2). Although the terminal allyls of the green 1(b=en,ex)(t=en_2) are bound more weakly, this isomer is still thermodynamically most stable. Structural data support this, since its longer terminal allyl Mo–C(o) and Mo–C(i) bonds are counterbalanced by bridging allyl Mo–C(o) and Mo–C(i) bond distances that are significantly shorter. Further evidence for stronger bonding of the bridging allyls in green 1(b=en,ex)(t=en_2) is derived from the fact that its Mo–Mo quadruple bond is longer (weaker) than that of the violet 1(b=en_2)(t=en_2). The shorter bridging allyl Mo–C(o) and Mo–C(i) bond distances in the green isomer allow more efficient overlap of the Mo–Mo π orbitals with the allylic π^* orbitals.[15] The enhanced metal to ligand π backbonding that results therefrom weakens the Mo–Mo multiple bond of 1(b=en,ex)(t=en_2) relative to that of 1(b=en_2)(t=en_2).

(15) Chisholm, M. H.; Hampden-Smith, M. J.; Huffman, J. C. *J. Am. Chem. Soc.* **1988**, *110*, 4070.

The weaker bonding of the bridging allyls to the dimolybdenum center in the violet 1(b=en_2)(t=en_2) may be a further consequence of the inefficient packing of these bridging allyls. In general, the optimal angle between cis-oriented ligands for overlap with metal-centered d orbitals is 90°. The angle between the bridging allyls in 1(b=en,ex)(t=en_2) of 93° is significantly closer to this optimal angle than the corresponding angle in 1(b=en_2)(t=en_2) of 98.1°. Thus, the decreased packing efficiency of the bridging allyls in 1(b=en_2)(t=en_2) (see Figure 4) may also decrease the efficiency of their orbital overlap with the d orbitals of the dimolybdenum center. Mo_2 fragment orbitals utilized in bonding to the bridging allyls are also utilized in bonding to the terminal allyls. In order to compensate for the inefficient bonding of the bridging allyls in 1(b=en_2)(t=en_2), bonding to its terminal allyls is enhanced making them less susceptible to reagent attack relative to those in 1(b=en,ex)(t=en_2).

Synthesis and Isolation of $Mo_2(\mu_2\text{-}\eta^3\text{-methallyl})_2(\eta^3\text{-methallyl})_2$ (2). The reaction of $Mo_2(OAc)_4$ with 4 equiv of (2-methyl propenyl)magnesium chloride, i.e., methallyl Grignard, yields navy blue 2 in diethyl ether. The compound appears to be more sensitive to O_2 than 1 presumably due to the inductive effects of the methyls at the π-allylic meso positions.

Both 1 and 2 have a high affinity for nonpolar hydrocarbon solvents with that of the latter being greater. The parent molecule, 1, is readily purified by (a) the in vacuo removal of the reaction solvent, diethyl ether, (b) separation of 1 from residual reagents and polar byproducts via extraction with pentane, and (c) crystallization of 1 from pentane. The purity of the final product is not highly dependent on the stoichiometry or purity of the reagents used. This is not true for 2. Significant concentrations of methallyl Grignard are extractable into pentane; thus, $Mo_2(OAc)_4$ must be used in a slight excess. Furthermore, nonvolatile 2,5-dimethyl-1,5-hexadiene often accompanies methallyl Grignard as an impurity. Attempts to crystallize 2 from pentane in the presence of significant quantities of the diene impurity have failed due to the total affinity of 2 for this "solvent" mixture. Therefore, methallyl Grignard must be synthesized very carefully in order to deter formation of 2,5-dimethyl-1,5-hexadiene.[16]

Although we have obtained samples of 2 virtually free of methallyl Grignard and 2,5-dimethyl-1,5-hexadiene, attempts, thus far, to obtain crystals suitable for X-ray crystallography have failed. However, the intricate ^1H NMR spectrum of 2 contains sufficient information to allow its structural elucidation. As with 1, 2 exists in solution as a mixture of isomers. We have been able to identify two isomers of 2 by utilizing ^1H–^1H COSY plots of both 1 and 2, along with the NOE-derived assignments for 1 reported by Benn et al.[11] as described below.

^1H NMR Patterns for Allyl Configurations in $M_2(\mu_2\text{-}\eta^3\text{-allyl})_2(\eta^3\text{-allyl})_2$ Complexes. Benn et al.[11] have assigned peaks for 1(b=en,ex)(t=en_2) and 1(b=en,ex)(t=en,ex) as well as the corresponding isomers for the isostructural $Cr_2(\mu_2\text{-}\eta^3\text{-allyl})_2(\eta^3\text{-allyl})_2$ (3) utilizing difference NOE (nuclear Overhauser effect) methods. Peaks corresponding to meso, syn, and anti protons in allylic ^1H NMR patterns were differentiated by using the magnitude of vicinal coupling constants, $^3J(^1H_{meso}\text{–}^1H_{anti}) > {}^3J(^1H_{meso}\text{–}^1H_{syn})$. Assignments of the various allylic ^1H NMR patterns to the correct binding mode (η^3-allyl vs μ_2-η^3-allyl) and configuration (endo vs exo) were augmented by crystal structures of the major isomer in solution, 1(b=en,ex)(t=en_2)[10] and 3(b=en,ex)(t=en_2),[17] respectively. Actual structural assignments to each allylic NMR pattern were made on the basis of inter-allyl NOEs. The major isomers of 1 and 3 contain a mirror plane and exhibit 11 proton resonances. The minor isomers, 1(b=en,ex)(t=en,ex) and 3(b=en,ex)(t=en,ex), are chiral and are characterized by 20 proton resonances.

In the major and minor isomers of both 1 and 3, two distinctive patterns are found in the strength and nature of the proton–proton couplings reported by Benn et al.[11] When compared to the bridging allyls, the terminal allyls tend to have stronger intra-allyl ^1H–^1H coupling. The meso–anti (14–16 Hz) and meso–syn (8–9 Hz) coupling constants for terminal allyls are larger than those observed for bridging allyls, 11–13 and 6–7.5 Hz, respectively. Evidence for stronger *intra*allyl coupling for terminal allyls can also be derived from the ^1H–^1H COSY of 1 at 200 MHz (Figure 1b). For the minor isomer, 1(b=en,ex)(t=en,ex), both syn–syn and anti–anti crosspeaks are observed for terminal allyls. Only syn–syn crosspeaks are observed for bridging allyls. For the major isomer, 1(b=en,ex)(t=en_2), a similar pattern is observed for terminal allyls whereas the bridging allyls are bisected by a mirror plane causing equivalency of their syn–syn and anti–anti proton pairs. However, a set of crosspeaks indicate *inter*-allyl ^1H–^1H coupling between the anti protons of the exo and endo bridging allyls. This inter-allyl coupling is through a minimum of four bonds, ^4J(H–C–Mo–C′–H′). Since even the strongest crosspeaks corresponding to the minor isomer, 1(b=en,ex)(t=en,ex), are faint, its inter-allyl coupling could not be detected. Inter-allyl coupling between two terminal allyls is expected to be much weaker because such coupling must occur through a minimum of five bonds, ^5J(H–C–Mo–Mo′–C′–H′). In summary, terminal allyls exhibit a larger number of detectable *intra*-allyl crosspeaks than their bridging counterparts whereas the latter exhibit *inter*-allyl crosspeaks.

The chemical shift range for the allylic proton resonances in 1 and 3 is extraordinary: 7.5–2.5 and 4.0–0.0 ppm for meso and methylenic protons, respectively (see Table II). This variability in chemical shift is due in part to the following two factors: (a) Each of the C–H bonds are tangential to the electron cloud of the dimetal center. Thus, their position relative to this anisotropic electron cloud will effect their proton chemical shift. (b) Each C–H bond will be effected to a varying extent by the π-electron clouds of neighboring allyls.

Distinctive chemical shift patterns are observed for each η^3-allyl bonding mode. Although the relative positions of resonances corresponding to isostructural protons vary somewhat between M = Mo and M = Cr, there is a very good correlation between chemical shift patterns corresponding to allyls with identical configurations on different isomers containing the same dimetal center. The wide range of chemical shifts allow differentiation of *endo*- or *exo*-allyl configurations through such correlations. For exo-bridging and endo-terminal configurations, syn resonances are *downfield* of their anti counterparts, whereas for endo-bridging and exo-terminal configurations, syn resonances are *upfield* of their anti counterparts.

^1H NMR Characterization of 2(b=en,ex)(t=en,ex). The major isomer of 2 is isostructural with the minor isomer of 1, 1(b=en,ex)(t=en,ex): evidence for four independent allylic fragments is observed in its COSY spectrum corresponding to a total of 20 resonances. No other structural isomer has a lower degree of symmetry. Because

(16) Lehmkuhl, H.; Bergstein, W. *Justus Liebigs Ann. Chem.* **1978**, 1436.

(17) Aoki, T.; Furosaki, A.; Tomiie, Y.; Ono, K.; Tanaka, K. *Bull. Chem. Soc. Jpn.* **1969**, *42*, 545.

Table II. Chemical Shift Data (ppm) for Isomers of 1 and 2

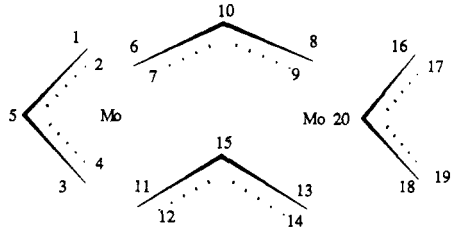

	isomer[a] (bridging allyls; terminal allyls)				
	1[b] (en,ex; en,en)	1[b] (en,ex; en,ex)	1 (en,en; en,en)	2 (en,ex; en,ex)	2 (en,ex; ex,ex)
	Exo-Terminal Allyl(s)				
1 (syn)		1.10		1.90	1.90
2 (anti)		3.10		2.63	2.49
3 (syn)		1.52		2.16	2.16
4 (anti)		3.42		3.54	3.73
5 (meso/CH_3)		4.38		0.69	0.66
	Endo-Terminal Allyl(s)				
16 (syn)	3.49	2.60	3.46	2.91	
17 (anti)	1.44	1.92	1.42	0.98	
18 (syn)	3.87	3.92		3.49	
19 (anti)	0.70	2.16		1.31	
20 (meso/CH_3)	3.99	4.35	3.38	1.12	
	Exo-Bridging Allyl				
6 (syn)	3.38	3.31		3.98	
7 (anti)	0.77	0.12		−0.15	
8 (syn)	3.38	3.31		3.80	3.84
9 (anti)	0.77	1.03		0.58	0.04
10 (meso/CH_3)	6.42	6.25		2.74	2.66
	Endo-Bridging Allyl(s)				
11 (syn)	1.31	0.92	1.34	1.12	
12 (anti)	3.10	2.75	3.20	3.09	
13 (syn)	1.31	1.64		1.57	1.31
14 (anti)	3.10	3.31		3.56	3.26
15 (meso/CH_3)	2.72	2.70	4.37	1.31	1.24

[a] The structure of each isomer is denoted by abbreviations for the configuration of the bridging and terminal allyls that are found in the first and second succeeding rows, respectively: en = endo and ex = exo. [b] These chemical shift data were obtained from ref 11.

of this, the above information is sufficient for the characterization of 2(b=en,ex)(t=en,ex). However, certain aspects of its COSY spectrum are notable and will be discussed here. An in depth analysis is found in the supplementary material.

As opposed to 1 where $^3J(^1H–^1H)$ couplings between the meso and syn or anti protons are the largest coupling constants (6–15 Hz), $^4J(^1H–^1H)$ ranging from 0–3 Hz and geminal ^2J ($^1H–^1H$) coupling constants that range between 1.5 and 3.0 Hz are expected for 2. Although such small coupling constants are often not resolved in one-dimensional ^1H NMR spectrum of 2, several of these couplings can be observed via crosspeaks in its COSY spectrum.

As with 1, the methallylic fragments of 2(b=en,ex)(t=en,ex) can be separated into two groups according to bonding mode. Intra-methallyl coupling is more pronounced for the terminal methallyls. For example, crosspeaks due to coupling of both syn and anti protons with methyl protons are observed for the terminal methallyls but not for their bridging counterparts. The crosspeak patterns for the bridging methallyls contain not only two pairs of distinct crosspeaks for four-bond *exo*-methallyl-*anti* to *endo*-methallyl-*anti* couplings, ^4J(H–C–Mo–C′–H′), but also two pairs of faint crosspeaks corresponding to five-bond *exo*-methallyl-*anti* to *endo*-methallyl-*anti* couplings [^5J(H–C–Mo–Mo′–C′–H′) + ^5J(H–C–C_{meso}–Mo′–C′–H′].

Very good correlations are observed between the chemical shift patterns of the endo-bridging, exo-bridging, and endo-terminal allyls/methallyls of 1 and 2(b=en,ex)(t=en,ex) (compare Table II). The large difference in chemical shift (1.18 ppm) between the resonances at 3.54 and 2.63 ppm due to the two anti protons of the exo-terminal allyl of 2(b=en,ex)(t=en,ex) relative to that observed (0.32 ppm) for the corresponding resonances at 3.42 and 3.10 ppm of 1(b=en,ex)(t=en,ex) may be due to an anisotropically induced upfield shift for the resonance at 2.63 ppm due to steric interactions between the corresponding proton and the methyl group of the exo-bridging methallyl.

^1H NMR Characterization of 2(b=en,ex)(t=ex$_2$). The crosspeak patterns corresponding to the minor isomer of 2 suggest that it contains two symmetrically related terminal methallyls and two types of bridging methallyls. The methylenic groups of each of the bridging groups are chemically equivalent. Its resonances correspond very closely in chemical shift to those of the endo-bridging, exo-bridging, and exo-terminal methallyls of 2(b=en,ex)(t=en,ex) (see Table II). Thus, this isomer, 2(b=en,ex)(t=ex$_2$), contains two exo-terminal allyls. Although 1(b=en,ex)(t=en$_2$) with two endo-terminal isomers is energetically most stable, steric interactions of two inward pointing methyl groups prevent formation of its isostructural analogue in 2. Thus, 2(b=en,ex)(t=en,ex) is the most stable isomer of 2 followed by 2(b=en,ex)(t=ex$_2$) with equilibrium abundances of 88% and 12%, respectively.

Conclusions

A number of observations pertinent to the preparation, characterization, and utility of compounds containing allylic ligands coordinated to dimetal centers have been made.

Configurational changes of bridging allyls in 1 and related molybdenum dimers occur very slowly. However, the addition of a "nonreactive" Lewis base such as pyridine catalyzes isomerization presumably by inducing a μ_2-η^3-allyl to η^1-allyl transformation. The reactivity of 1 was found to be very sensitive to the configuration of the bridging allyls and we propose that the increased kinetic stability of 1(b=en$_2$)(t=en$_2$) relative to 1(b=en,ex)(t=en$_2$) is a result of intensified interligand steric interactions in the former. In fact, the discovery of the less reactive 1(b=en$_2$)(t=en$_2$) has brought to light the cause of unexpected product distributions. For example, the addition of 2.0 equiv of acetylacetone to hydrocarbon solutions of 1 yield a mixture of unreacted violet 1(b=en$_2$)(t=en$_2$), the expected product, $Mo_2(\mu_2$-η^3-allyl$)_2(\eta^2$-acac$)_2$, and a product resulting from the protonation of a bridging allyl of $Mo_2(\mu_2$-η^3-allyl$)_2$-$(\eta^2$-acac$)_2$ by acetylacetone. The formation of the latter compound is prevented by assuming that the violet 1(b=en$_2$)(t=en$_2$) is inert and adjusting the stoichiometry of the reaction accordingly.

Trends in crosspeak patterns in the COSY spectra of 1 and 2 have allowed the differentiation of bridging and terminal allyls. This information coupled with chemical shift patterns has allowed the assignment of exo or endo configurations. These trends in chemical shifts and coupling patterns will be valuable tools in the elucidation of further structures containing allyls coordinated to a dimetal center.

Experimental Section

General Considerations. All reactions were carried out under a dry and oxygen-free atmosphere of N_2 by using standard Schlenk techniques. Samples were handled in a Vacuum Atmospheres Co. Dry Lab System. Pentane and hexane were refluxed over Na–K alloy for at least 16 h before use. Diethyl ether was dried

over sodium benzophenone ketyl. All solvents were collected and stored over 3-Å molecular sieves. Organic reagents were procured commercially and purged with nitrogen before use. Molybdenum hexacarbonyl was purchased from Pressure Chemical. Tetrakis(acetato)dimolybdenum,[18] methallylmagnesium chloride, and allylmagnesium chloride[19] were prepared according to literature procedures. Tetraallyldimolybdenum can be synthesized by utilizing $MoCl_5$,[4] $MoCl_3$,[20] or $Mo_2(OOCCH_3)_4$[7] as the molybdenum source. The latter method was found to be most suitable for this application. Anal. Calcd for $C_{12}H_{20}Mo_2$: C, 40.47; H, 5.66. Found: C, 40.32; H, 5.65. Figure 3 was created by utilizing graphics hardware and software belonging to Dr. Dennis S. Marynick.

Physical Techniques. NMR spectra were recorded on a Nicolet NT-200 spectrometer at 200 and 50 MHz for ^1H and ^{13}C, respectively, with C_6D_6 as the solvent. All ^1H NMR chemical shifts are in ppm relative to the C_6D_5H singlet set at 7.13 ppm, whereas ^{13}C chemical shifts are relative to the C_6D_6 triplet at 128.0 ppm. Difference homodecoupling spectroscopy was utilized in tandem with COSY experiments to resolve ^1H–^1H coupling for more complicated spectra with overlapping multiplets.[21] The data for COSY experiments were acquired with a 90° secondary pulse and were calculated from a sequence of 512 1K spectra. The 90° pulse was determined experimentally prior to each acquisition. Elemental analyses were performed by Texas Analytical Laboratories, Tallahassee, FL.

Isolation of 1(b=en$_2$)(t=en$_2$). Approximately 350 mL of a 0.32 M solution (130 mmol) of allylMgCl in diethyl ether was introduced under nitrogen into a three-neck, 1000-mL round-bottom flask. This solution was diluted with an additional 100 mL of diethyl ether and stirred at 0 °C while 8.5 g (20 mmol) of $Mo_2(OAc)_4$ was added over a period of 2 h. At the end of this addition, the solution was a dark green. The flask was kept at ice temperature and stirred for 16 h. The ether was removed in vacuo, leaving a powdery green residue. The residue was extracted with pentane in five successive 50–75-mL portions, and the extract was filtered through Celite into a 500-mL round-bottom flask. The contents of this flask were then titrated with less than 0.6 mL of methanol to a dark purple color. This solution was filtered through Celite into a 500-mL round-bottom flask, and most of the pentane was removed in vacuo. This concentrated solution was cooled to −50 C, and after 15 h, a violet microcrystalline solid was collected. The overall yield was 0.24 g, or 3.4%. ^1H NMR: Refer to Table II for chemical shifts. ^1H–^1H coupling (Hz): μ_2-η^3-allyl $^3J(H_{meso}\text{–}H_{anti})$ = 11.0 Hz, $^3J(H_{meso}\text{–}H_{syn})$ = 7.1 Hz, $^2J + {}^4J(H_{syn}\text{–}H_{anti})$ = 4.7 Hz; η^3-allyl $^3J(H_{meso}\text{–}H_{anti})$ = 12.9 Hz, $^3J(H_{meso}\text{–}H_{syb})$ = 7.5 Hz, $^2J + {}^4J(H_{syn}\text{–}H_{anti})$ = 1.8 Hz. ^{13}C NMR (chemical shifts in ppm): η^3-allyl C_{meso} 120.8, $C_{methylene}$ 66.1; μ_2-η^3-allyl C_{meso} 80.3, $C_{methylene}$ 46.5.

X-ray Crystallography. Carbon monoxide (5–6 equiv) was added via gastight syringe to 0.5 g (1.4 mmol) of 1 in 80 mL of pentane at 18–20 °C. The color of the solution changed from green to violet. The solution was then filtered through Celite, and the volume of filtrate was reduced to 10–15 mL in vacuo. Crystallization at −15 °C over 24 h provided violet hexagonal crystals (0.25 mm × 0.35 mm).

Crystal data for 1(b=en$_2$)(t=en$_2$), $C_{12}H_{20}Mo_2$, were collected at 213 K, using an automatic Nicolet R3m/V diffractometer and Mo Kα radiation. The complex crystallizes in the orthorhombic space group *Pbcn* with cell constants a = 8.275 (11) Å, b = 11.832 (7) Å, c = 12.862 (9) Å, V = 1259 (2) Å^3, Z = 8, and $R(F)$ = 3.01%. A total of 1119 independent reflections in the range $3.0 \le 2\theta \le 50.0°$ were collected. Three standard reflections were collected after every 100 reflections. The structure was solved by direct methods programs used in SHELXTL-PLUS (Sheldrick, G. M. *Structure Determination Software Programs*; Nicolet Instrument Corp.: Madison, WI, 1988) and subsequent difference Fourier methods. Final full-matrix least-squares refinement (SHELXTL-PLUS) using 816 observed reflections with $F > 6.0\sigma(F)$ converged to R = 0.030 and R_w = 0.038. All non-H atoms were refined anisotropically. All hydrogen atoms were placed into calculated positions with fixed isotropic temperature factors. The function being minimized was $\sum w(F_o - F_c)^2$ with the weight used being $w^{-1} = \sigma^2(F) + 0.0040F^2$. Scattering factors for C, H, and Mo were those stored in SHELXTL-PLUS.

There are eight equivalent positions in the *Pbcn* unit cell defining four molecular positions for 1(b=en$_2$)(t=en$_2$). A disorder in the molecular packing exists such that two distinct molecular orientations, A and B, with equal probability are observed at each of the four molecular positions in the *Pbcn* crystal lattice. Thus, molecular orientations A and B occupy the same region of space in the unit cell but differ in orientation such that their Mo–Mo bond axes are mutually orthogonal and the atomic positions for the *terminal* allyl carbon atoms for the molecule in orientation A are accidentally coincident with the *bridging* allyl carbon atoms of the molecule in orientation B and vice versa.

The structure was solved by successfully utilizing a 50% occupancy at each of the four molybdenum atom sites belonging to orientation A and B. The positions of the carbon atoms were solved by utilizing a simplifying assumption. For example, three carbon sites were solved as belonging 100% to the terminal allyl carbons for orientation A instead of being occupied 50% by the terminal allyl carbons of orientation A and 50% by the bridging allyl carbons of orientation B. Similarly, the three other independent carbon sites were solved as belonging 100% to the bridging allyl carbons of orientation A instead of being occupied 50% by the bridging allyl carbons of orientation A and the terminal allyl carbons of orientation B. Very little residual electron density was observed by solving the structure in this manner, confirming the fact that each set of two 50% occupied carbon positions are indeed almost exactly coincident.

Quantitative Analysis of Reaction of Methanol with 1. The addition of 4.0 μL (95.7 μmol) of methanol to 0.21 g (0.590 mmol) of 1 at 5 °C caused the formation of a brown precipitate and a turquois solution. The solution was separated from the brown solid by using a preweighed disposable pipet filled chronologically with a small wad of glass wool, a small amount of predried alumina, 4 cm of predried Celite, and another small wad of glass wool. Prior to loading, the top of the pipet was melted carefully, forming a bead to prevent a 9-mm septum from slipping off after it was fastened with a wire. The suspension was transferred to the pipet via a small-bore Teflon cannula. After the filter was dried in an oven overnight, the weight increase of the pipet filter was 0.0369 g. Assuming the weight of the brown solid remains essentially constant upon exposure to air, the weight gain of the pipet is equivalent to a 1:1 reaction of methanol with 1. The violet 1(b=en$_2$)(t=en$_2$) increased from 25% to 31% of the isomer distribution after the addition of the methanol, which was also consistent with a 1:1 methanol reaction. The pre- and postreaction ratios 1(b=en,ex)(t=en$_2$):1(b=en$_2$)(t=en$_2$):1(b=en,ex)(t=en,ex), were determined by "cut and weigh" integration of highly expanded ^1H NMR resonances at 6.42, 4.37, and 6.25 ppm, respectively.

Lewis Base Catalyzed Isomerization of 1(b=en$_2$)(t=en$_2$). A sample of isomerically pure 1(b=en$_2$)(t=en$_2$) was dissolved in 0.5 mL of benzene-d_6 in a 5-mm-diameter NMR tube with a septum cap. An excess of pyridine was added via a microliter syringe, and the ^1H NMR spectrum was monitored periodically to determine the extent of isomerization. Alternatively, a solution of bis(diphenylphosphino)methane in benzene-d_6 was added via a Teflon cannula to an NMR tube containing a 1(b=en$_2$)(t=en$_2$) solution. Again, the extent of isomerization was determined by ^1H NMR spectroscopy.

$Mo_2(\mu_2\text{-}\eta^3\text{-methallyl})_2(\eta^3\text{-methallyl})_2$ (2). $Mo_2(OOCCH_3)_4$ (2.2 g, 5.1 mmol) was placed in a solid addition tube under vacuum for 0.5 h and then placed under nitrogen. This was slowly added to a 500-mL round-bottom three-neck flask with a nitrogen inlet containing a stirred solution with 3.2 equiv (16.5 mmol) of methallylmagnesium chloride in ether (250 mL), over a 1 h period at 0 °C. The solution was then allowed to warm to room temperature for 1 h. The ether was stripped from the solution. The solid was then extracted with pentane (three 50-mL portions), and the extract was filtered through Celite. The pentane was stripped from this solution to yield 0.8 g (38% yield) of a dark blue powder. Due to its high solubility, all attempts to obtain

(18) Brignole, A. B.; Cotton, F. A. *Inorg. Synth.* **1972**, *13*, 87.
(19) Grummitt, O.; Budewitz, E. P.; Chudd, C. C. *Org. Synth.* **1963**, *4*, 751.
(20) Blau, R. J.; Papadopoulou, O. V.; Tsay, R.-J. Unpublished results.
(21) Sanders, J. K. M.; Hunter, B. K. *Modern NMR Spectroscopy: A Guide for Chemists*; Oxford University Press: New York, 1970; pp 540–557, 138–150.

a solid precipitate of **2** from pentane with an acceptable elemental analysis have failed. A common contaminant is 2,5-dimethyl-1,5-hexadiene, an impurity originating from the synthesis of C_4H_7MgCl. If this nonvolatile hydrocarbon is present in high concentrations, a dark blue oil will be obtained. ^1H NMR: Refer to Table II.

Acknowledgment. This work was supported by grants from the Robert A. Welch Foundation (Y-1076) and the donors of the Petroleum Research Fund, administered by the American Chemical Society. The efforts of a Research Assistant, Mrs. Su-Inn Ho, are also gratefully acknowledged.

Supplementary Material Available: A structure determination listing, tables of positional and isotropic thermal parameters (Table 1), bond lengths (Table 2), bond angles (Table 3), anisotropic temperature factors (Table 4), and H coordinates and isotropic displacement parameters (Table 5), and a peak by peak analysis of the COSY plots for **1** and **2** (20 pages); a listing of observed and calculated structure factors (Table 6) (4 pages). Ordering information is given on any current masthead page.

Mechanism of Isomerization of Alkylidene Complexes $[(\eta^5\text{-}C_5H_5)Re(NO)(PPh_3)(=CRCHR'R'')]^+X^-$ to Alkene Complexes $[(\eta^5\text{-}C_5H_5)Re(NO)(PPh_3)(RHC=CR'R'')]^+X^-$: An Organometallic Wagner–Meerwein-Type Rearrangement

Christophe Roger, Gerardo S. Bodner, William G. Hatton, and J. A. Gladysz*

Department of Chemistry, University of Utah, Salt Lake City, Utah 84112

Received March 20, 1991

Propylidene complex $[(\eta^5\text{-}C_5H_5)Re(NO)(PPh_3)(=CHCH_2CH_3)]^+PF_6^-$ (**1c**$^+PF_6^-$) cleanly rearranges to propene complex $[(\eta^5\text{-}C_5H_5)Re(NO)(PPh_3)(H_2C=CHCH_3)]^+PF_6^-$ (C_6D_5Cl, 65–86 °C; $\Delta H^\ddagger = 27 \pm 1$ kcal/mol; $\Delta S^\ddagger = 3 \pm 3$ eu). Experiments with deuterated **1c**$^+PF_6^-$ show a modest primary kinetic deuterium isotope effect ($k(=CHCH_2CH_3)/k(=CHCD_2CH_3)$ = 1.95–1.40) but a considerable inverse secondary kinetic deuterium isotope effect ($k(Re=CH)/k(Re=CD)$ = 0.50–0.58). A crossover experiment shows intramolecular hydride migration and the absence of PPh_3 ligand dissociation. Optically active **1c**$^+PF_6^-$ rearranges with retention of configuration at rhenium, but the hydride shift is not stereospecific at the migration terminus. However, the rearrangement of isobutylidene complex $[(\eta^5\text{-}C_5H_5)Re(NO)(PPh_3)(=CHCH(CH_3)_2)]^+SO_3F^-$ to isobutylene complex $[(\eta^5\text{-}C_5H_5)Re(NO)(PPh_3)(H_2C=C(CH_3)_2)]^+SO_3F^-$ is highly stereoselective at the migration origin and terminus, and much faster than that of **1c**$^+PF_6^-$ (CD_2Cl_2, 3–25 °C; $\Delta H^\ddagger = 21 \pm 1$ kcal/mol; $\Delta S^\ddagger = -3 \pm 3$ eu). Rearrangements of analogous pentylidene and cyclopentylidene complexes are also studied. An orbital symmetry analysis of these reactions is given.

Carbon–hydrogen bond activation is a focal point of research in organometallic chemistry. Several classes of hydrocarbon ligands have been found to participate in prototropic rearrangements near room temperature. For example, alkylidene complexes often undergo a 1,2-hydride migration to give alkene complexes (eq i).[1-10] Also, terminal alkyne complexes have been observed to rearrange to vinylidene complexes (eq ii).[11-13] Interestingly, eq i (M=C → π) has a thermodynamic sense opposite to that of eq ii (π → M=C).

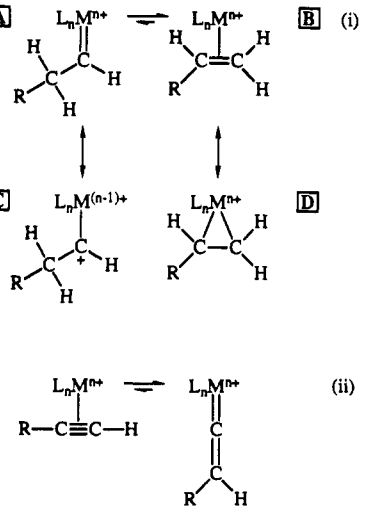

(1) Brookhart, M.; Tucker, J. R.; Husk, G. R. *J. Am. Chem. Soc.* **1981**, *103*, 979; **1983**, *105*, 258.
(2) Marsella, J. A.; Folting, K.; Huffman, J. C.; Caulton, K. G. *J. Am. Chem. Soc.* **1981**, *103*, 5596.
(3) Bodnar, T.; Cutler, A. R. *J. Organomet. Chem.* **1981**, *213*, C31.
(4) Casey, C. P.; Miles, W. H.; Tukada, H. *J. Am. Chem. Soc.* **1985**, *107*, 2924.
(5) (a) Kremer, K. A. M.; Kuo, G.-H.; O'Connor, E. J.; Helquist, P.; Kerber, R. C. *J. Am. Chem. Soc.* **1982**, *104*, 6119. (b) Kuo, G.-H.; Helquist, P.; Kerber, R. C. *Organometallics* **1984**, *3*, 806.
(6) Hatton, W. G.; Gladysz, J. A. *J. Am. Chem. Soc.* **1983**, *105*, 6157.
(7) Freudenberger, J. H.; Schrock, R. R. *Organometallics* **1985**, *4*, 1937.
(8) Examples where the alkylidene complex is not directly observed: (a) Cutler, A.; Fish, R. W.; Giering, W. P.; Rosenblum, M. *J. Am. Chem. Soc.* **1972**, *94*, 4354. (b) Labinger, J. A.; Schwartz, J. *Ibid.* **1975**, *97*, 1596. (c) Casey, C. P.; Albin, L. D.; Burkhardt, T. J. *Ibid.* **1977**, *99*, 2533. (d) Fischer, E. O.; Held, W. *J. Organomet. Chem.* **1976**, *112*, C59. (e) Guerchais, V. *J. Chem. Soc., Chem. Commun.* **1990**, 534.
(9) Some conceptually related hydride migrations: (a) Casey, C. P.; Marder, S. R.; Adams, B. R. *J. Am. Chem. Soc.* **1985**, *107*, 7700. (b) Green, M.; Orpen, A. G.; Schaverein, C. J. *J. Chem. Soc., Chem. Commun.* **1984**, 37.
(10) Some analogous carbon migrations: (a) Bly, R. S.; Bly, R. K. *J. Chem. Soc., Chem. Commun.* **1986**, 1046. (b) Bly, R. S.; Bly, R. K.; Hossain, M. M.; Lebioda, L.; Raja, M. *J. Am. Chem. Soc.* **1988**, *110*, 7723. (c) Bly, R. S.; Silverman, G. S.; Bly, R. K. *Ibid.* **1988**, *110*, 7730. (d) Bly, R. S.; Wu, R.; Bly, R. K. *Organometallics* **1990**, *9*, 936. (e) Bly, R. S.; Raja, M. *Ibid.* **1990**, *9*, 1500.
(11) (a) Bruce, M. I. *Chem. Rev.* **1991**, *91*, 197. (b) Silvestre, J.; Hoffmann, R. *Helv. Chim. Acta* **1985**, *68*, 1461. (c) Pombeiro, A. J. L.; Richards, R. L. *Coord. Chem. Rev.* **1990**, *104*, 13.
(12) (a) Bullock, R. M. *J. Chem. Soc., Chem. Commun.* **1989**, 165. (b) Werner, H. *Angew. Chem., Int. Ed. Engl.* **1990**, *29*, 1077. (c) Werner, H.; Hampp, A.; Peters, K.; Peters, E. M.; Walz, L.; von Schnering, H. G. *Z. Naturforsch.* **1990**, *45b*, 1548.
(13) Kowalczyk, J. J.; Arif, A. M.; Gladysz, J. A. *Organometallics* **1991**, *10*, 1079.

0276-7333/91/2310-3266$02.50/0